Electronic Supplementary Material (ESI) for ChemComm.
This journal is © The Royal Society of Chemistry 2019

Hydrothermal synthesis of novel rhombic dodecahedral SnS nanocrystals for highly efficient photothermal therapy

Fei Chen,[a†] Dongliang Yang,[b,c†] Haifeng Shen,[a] Meng Deng,[a] Ying Zhang,[b] Guolun Zhong,[a] Yanling Hu,[b] Lixing Weng,[d] Zhimin Luo[b*] and Lianhui Wang[b*]

[a] Laboratory of Polymer Materials and Engineering, Ningbo Institute of Technology, Zhejiang University, No.1 Qianhu South Road, Ningbo 315100, China.

[b] Key Laboratory for Organic Electronics and Information Displays & Jiangsu Key Laboratory for Biosensors, Institute of Advanced Materials (IAM), Jiangsu National Synergetic Innovation Center for Advanced Materials (SICAM), Nanjing University of Posts & Telecommunications, 9 Wenyuan Road, Nanjing 210023, China.

[c] School of Physical and Mathematical Sciences, Nanjing Tech University (NanjingTech), 30 South Puzhu Road, Nanjing 211816, China; Key Laboratory for Organic Electronics and Information Displays & Jiangsu Key Laboratory for Biosensors, Institute of Advanced Materials (IAM), Jiangsu National Synergetic Innovation Center for Advanced Materials (SICAM), Nanjing University of Posts and Telecommunications, 9 Wenyuan Road, Nanjing 210023, China.

[d] College of Geography and Biological Information, Nanjing University of Posts and Telecommunications, 9 Wenyuan Road, Nanjing 210023, China.

*Corresponding author. Email: iamlhwang@njupt.edu.cn.

[+]These authors contributed equally to this work.

Experimental Section

Materials

Tin(II) chloride dehydrate, L-cysteine, dimethyl sulfoxide (DMSO), polyvinylpyrrolidone (PVP) (M_w = 1300000), PVP K30 (M_w~40000) and PVP K90 (M_w = 360000) were purchased from Sigma-Aldrich (Saint Louis, Missouri, USA). Dulbecco's modified Eagle's medium (DMEM) was purchased from Fisher Scientific (a part of Thermo Fisher Scientific, Loughborough, UK). Milli-Q water (Milli-Q System, Millipore, Billerica, MA) was used in all experiments. All chemicals were used directly without further treatment.

The preparation of rhombic dodecahedral SnS nanocrystals (RD SnS NCs)

RD SnS NCs were synthesized via a hydrothermal method. In a typical procedure, 1 mmol of Tin(II) chloride dihydrate, 1 mmol of L-cysteine and 0.4 μmol of PVP (M_w~1300000), were added into 75 mL of distilled water, respectively. The resulting mixture was stirred for 2 h, and then transferred to a Teflon-lined stainless-autoclave, which was sealed and maintained at 200 ^{o}C for 110 min. After the reaction was finished and the solution was cooled to room temperature, the final product was collected through centrifugation, and washed with distilled water and ethanol for several times. The product was dried in vacuum drying oven and kept for further characterizations and applications.

Characterizations

The crystal structure was characterized by an X-ray diffractometer (D/max-2500, Rigaku) with a Cu target. UV-vis-NIR spectroscopy was collected on a UV–vis–NIR spectroscope (UV-3600, Shimadzu). The morphology and crystal structures were characterized by field emission scanning electron microscope (JSM-7600F, JEOL) and transmission electron microscope (JEOL JEM-2100F). X-ray photoelectron spectroscopy (XPS) was performed by using a PHI 5000 VersaProbe (Ulvac-Phi, Japan)

with Al Kα (hν=1486.6 eV) as the excitation source. The binding energies were calibrated by the C 1s peak at 284.6 eV. The concentration of RD SnS NCs was determined by Inductively Coupled Plasma Optical Emission Spectrometer (ICP-OES, Optima 5300DV, Perkin Elmer).

Hemolysis tests of RD SnS NCs

0.5 mL of blood sample obtained from mice was added to PBS (pH = 7.4, 10 mM), and then RBCs were collected by centrifugation at 1000 rpm for 5 min. After being washed with 6 mL PBS (pH = 7.4, 10 mM) for three times, the RBCs were suspended in 1 mL of PBS (pH = 7.4, 10 mM). Afterward, 100 μL of RBC suspension was mixed with 0.9 mL of RD SnS NCs suspension in PBS (pH = 7.4, 10 mM) and kept in 37 °C for 2 h. Besides, 100 μL of RBC suspension incubated with 0.9 mL of water or PBS (pH = 7.4, 10 mM) was used as the positive or negative control, respectively. Finally, the dispersions were centrifuged at 1000 rpm for 5 min, and 100 μL of supernatant was transferred to a 96-well plate. The absorbances of the supernatants at 540 nm were measured by using a microplate reader. The hemolysis of RBCs (%) was calculated by the ratio of the absorbance of the RBCs treated with RD SnS NCs to that of the cells incubated with water.

Cytotoxicity assay and photothermal therapy in vitro

Cell metabolic activity *in vitro* was measured using the methylthiazolyl tetrazolium (MTT) assay. 100 μL of *HeLa* cervical cancer cell (1×10^5 cells mL^{-1}) suspension was seeded into 96-well plate per well and incubated overnight. The culture medium was then removed and DMEM medium containing various concentrations of RD SnS NCs (0.6, 0.3, 0.06, 0.03, 0.006, 0.003 mg mL^{-1}) was added to the plate. After being incubated at 37 ℃ under 5% CO_2 for 24 h, each well was washed with PBS solution (pH = 7.4, 10 mM), then 20 μL of MTT (5.0 mg mL^{-1}) was added into each well and the plate was incubated at 37 °C for an additional 4 h. Afterward, the cell culture was replaced with 150 μL of DMSO

to dissolve the formazan crystals. Finally, the absorbance of each sample at 570 nm was recorded using a Microplate Spectrophotometer (PowerWave XS2, BIOTEK, US). The cell viability (%) was expressed by the mean absorbance value of treated cells divided by that of control cells × 100. To evaluate the mortality rate of *HeLa* cell under exposure to different power densities of 785 nm laser, a similar procedure was performed without the irradiation of 785 nm laser after treatment with RD SnS NCs overnight. Photothermal therapy was also confirmd by confocal fluorescence imaging. The *HeLa* cells seeded into confocal dish were incubated with/without RD SnS NCs (0.3 mg mL^{-1}) for 8 h, and then irradiated by 785 nm laser (0.8 W cm^{-2}) for 10 min. Afterwards, the cells were stained with PI and Calcein AM for 15 min and rinsed with PBS solution. Finally, fluorescent imaging of cells was obtained using Olympus FV1000 confocal microscope.

In vivo toxicity studies

BALB/c female mice (4-6 weeks old, 5 mice per group) were intravenously administrated with the RD SnS NCs at a dose of 25 mg kg^{-1} via the tail vein. The control group of mice was intravenously injected with equal volumes of PBS solution (pH=7.4, 10 mM). Blood samples were drawn via retro-orbital sinus puncture after treatment for 1 d. The mice were then euthanized after treatment for 1 and 14 d, and the organs (kidney, spleen, liver, lung, and heart,) were collected, fixed in 4% formaldehyde, and embedded in paraffin in the usual way. Finally, the organs were sliced and stained with hematoxylin and eosin, and observed under a microscope (IX71, Olympus, Japan).

Photothermal ablation of tumors in vivo

Twenty tumor-bearing (about 60 mm^3) nude female mice (body weight about 15 g) were randomly divided into four groups (5 mice per group) as follows: group I intratumorally injected with 25 μL of PBS; group II intratumorally injected with 25 μL of RD SnS NCs (2 mg mL^{-1}); group III treated with

785 nm laser (1 W cm^{-2}, 10 min); group IV intratumorally injected with 25 μL of RD SnS NCs and treatment with 785 nm laser (1 W cm^{-2}, 10 min). An infrared thermal camera was used to monitor the temperature changes of tumor surface. The body weights and tumor volumes after different treatments were recorded every day for two weeks. The tumor volumes were calculated as follows: volume = (tumor length) × (tumor width)^2/2. Relative tumor volume was expressed as V/V_0 (V_0 was the initial tumor volume). The tumor-bearing nude mice were killed after treatment for 1 d, and tumors were harvested, embedded in paraffin for histological studies.

All animal experiments were performed according to the ethical guidelines, principles, and protocols for the care and use of laboratory animals by Animal Studies Committee of Nanjing Medical University.

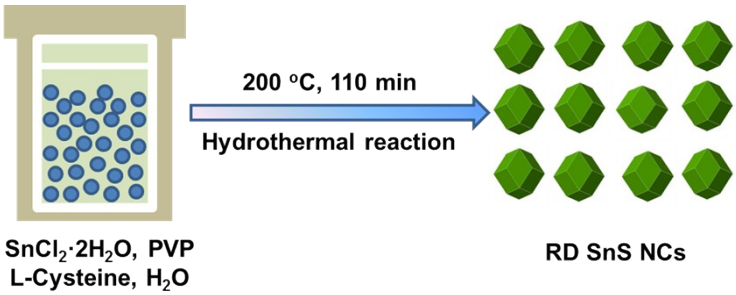

Scheme S1. One-pot hydrothermal synthesis of RD SnS NCs.

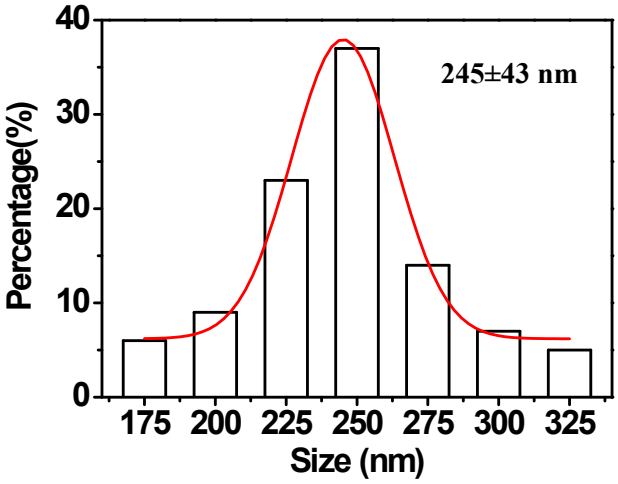

Figure S1. Size distribution of RD SnS NCs prepared with the reaction time of 110 min.

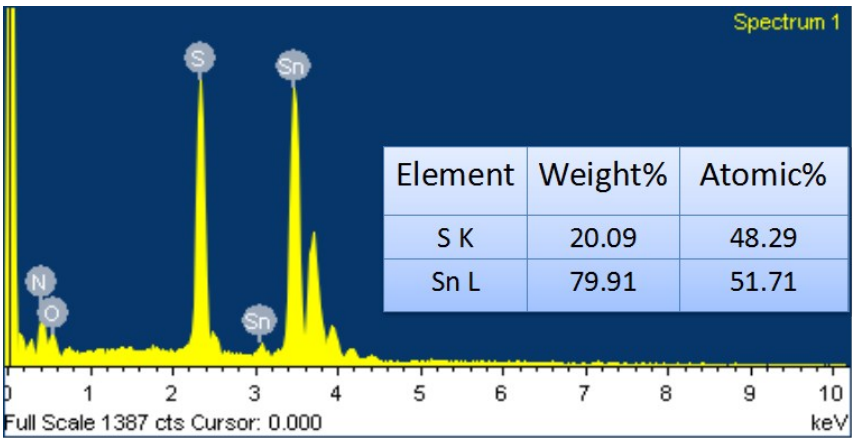

Figure S2. EDS characterization of RD SnS NCs.

Sn and S elements can be clearly observed from EDS characterization of RD SnS NCs (Figure S2), confirming their elemental compositions. The elemental ratio obtained from the EDS analysis is close to 1:1 (inset in Figure S2). The N and O elements are from PVP.

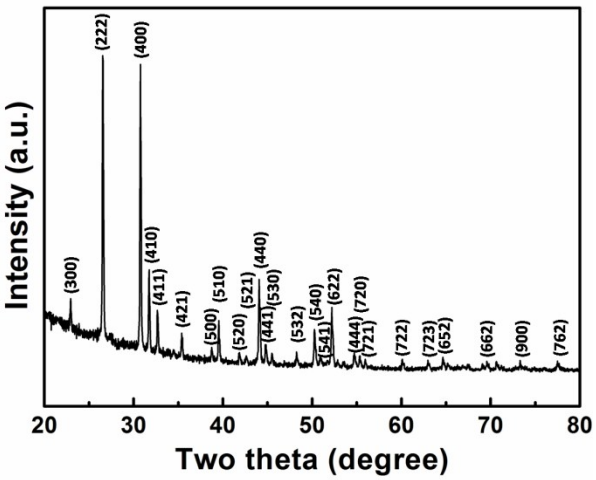

Figure S3. XRD pattern of RD SnS NCs.

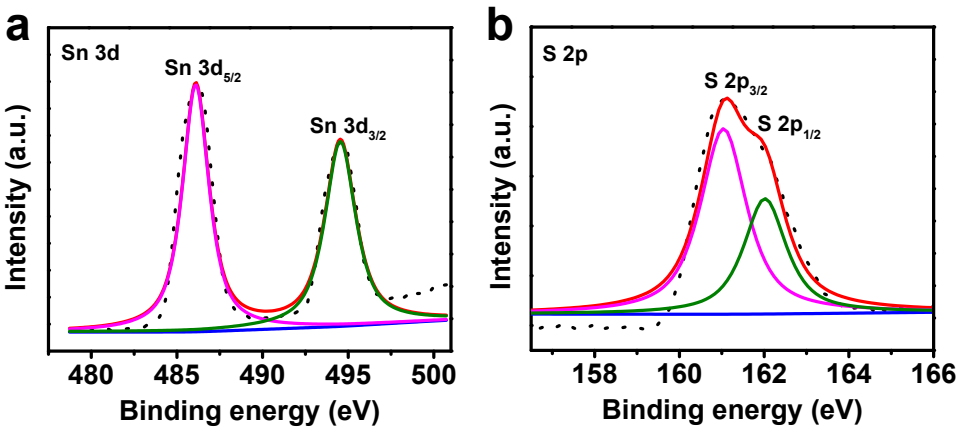

Figure S4. High-resolution XPS (a) Sn 3d, (b) S 2p spectra of RD SnS NCs.

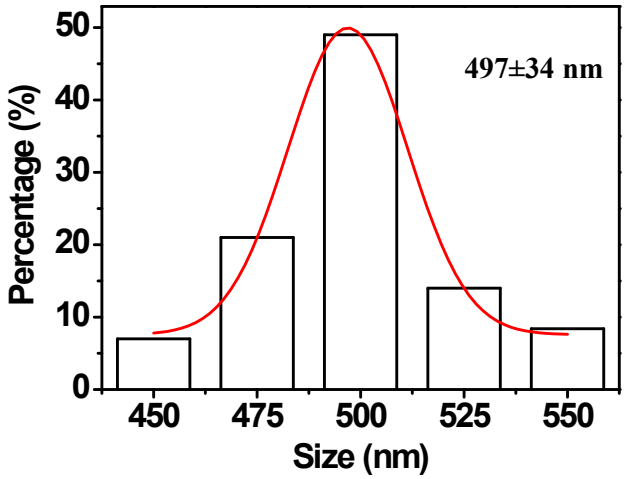

Figure S5. Size distribution of RD SnS NCs-2 prepared with the reaction time of 120 min.

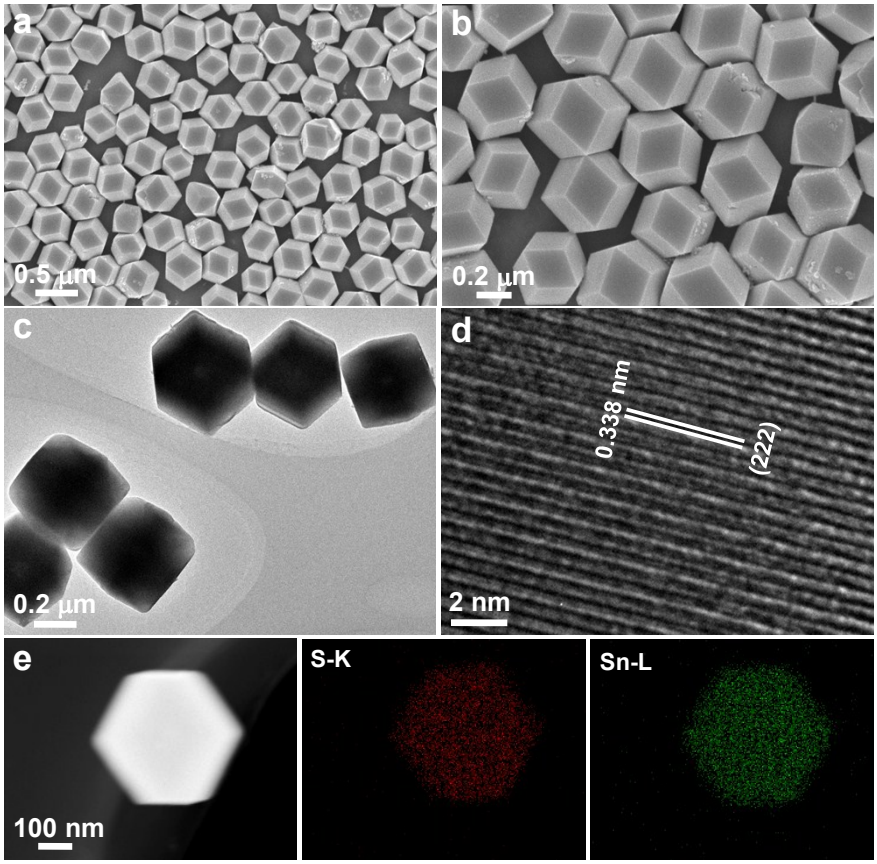

Figure S6. (a) SEM and (b) magnified SEM images of RD SnS NCs-2. (c) Low-magnification TEM and (d) HRTEM images of RD SnS NCs-2. (e) STEM image and its corresponding EDS elemental mapping of a RD SnS NC-2. Note that RD SnS NC-2 was prepared with the reaction time of 120 min.

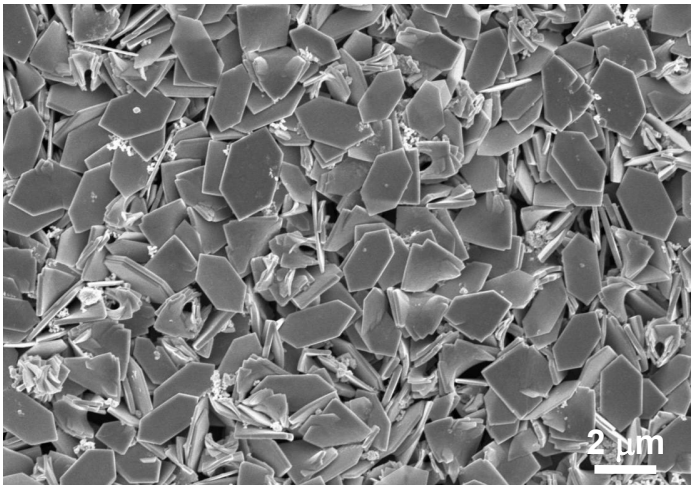

Figure S7. SEM image of hexagonal SnS nanocrystals obtained with the reaction time of 140 min.

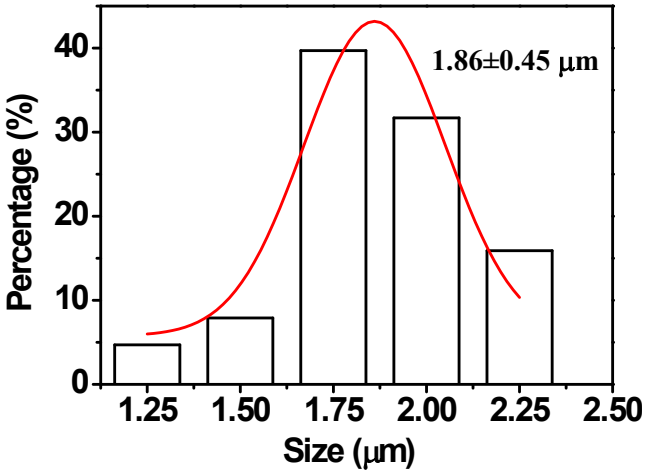

Figure S8. Size distribution of hexagonal SnS nanocrystals prepared with the reaction time of 140 min.

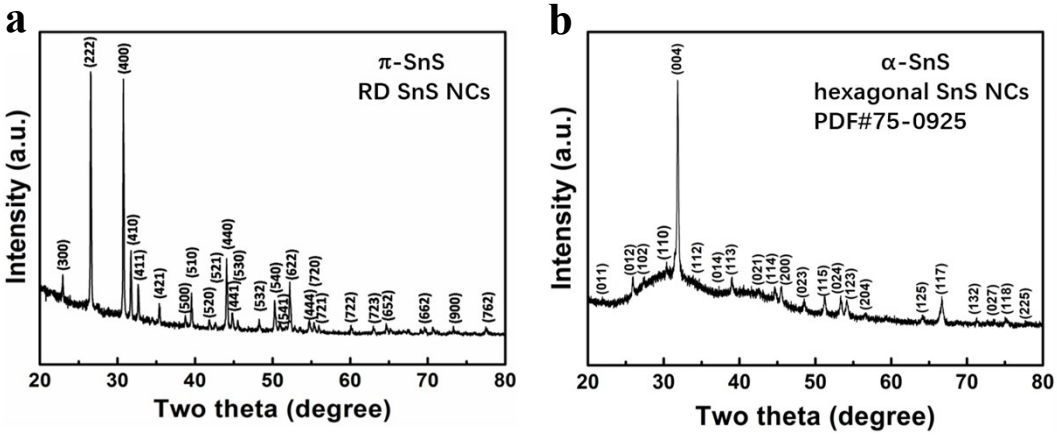

Figure S9. XRD patterns of (a) α-phase and (b) π-phase SnS phase.

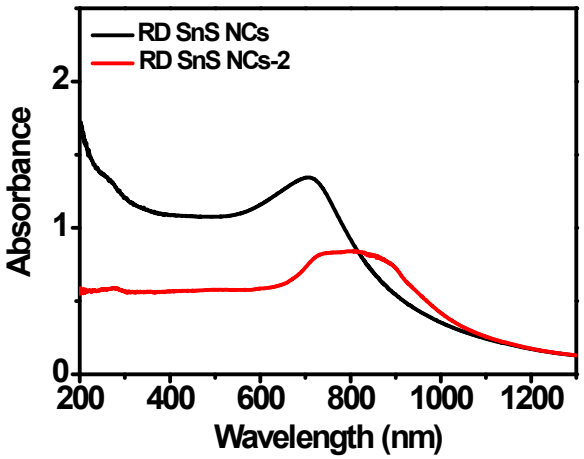

Figure S10. UV-vis-NIR spectroscopy of RD SnS NCs (245±43 nm) and RD SnS NCs-2 (497±34 nm).

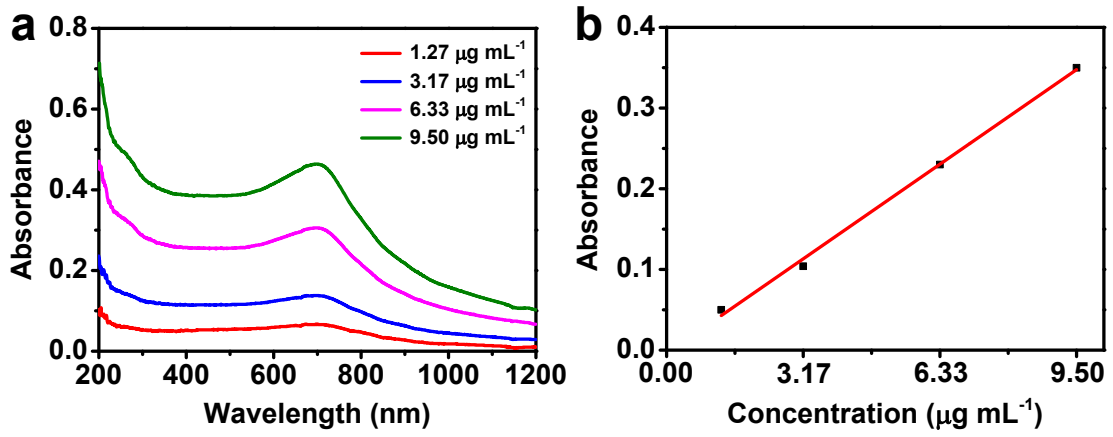

Figure S11. (a) UV-vis-NIR absorption spectra of RD SnS NCs (245±43 nm) with different concentrations (1.27, 3.17, 6.33, and 9.50 μg mL^{-1}). (b) The plot of absorbance at 785 nm versus the concentration of RD SnS NCs.

Measurements of extinction coefficient of RD SnS NCs

The mass extinction coefficient ε of RD SnS NCs can be calculated using the Beer-Lambert Law (Eq. 1). Here *A* is the absorbance of RD SnS NCs aqueous suspension at 785 nm, *L* is the length of the quartz cuvette (cm), *C* is the concentration of RD SnS NCs (g L^{-1}), ε is the extinction coefficient of RD SnS NCs.

$$\varepsilon = \frac{A}{LC} \qquad (1)$$

Calculation of photothermal conversion efficiency

According to Roper's and our previous report,[1, 2] the photothermal conversion coefficient (η) of RD SnS NCs can be calculated using Eq. 2:

$$\eta = \frac{hS(T_{Max} - T_{Surr}) - Q_0}{I(1 - 10^{-A})} \qquad (2)$$

where T_{Max} is the maximum temperature of RD SnS NCs aqueous suspension, T_{Surr} is the ambient temperature of surroundings, the (T_{Max}-T_{surr}) was 44. Q_0 is the energy absorbed by the sample vial, which can be measured using a PCR tube containing 100 μL of Mili-Q water without the RD SnS NCs (Q_0 =

16 mW). I is 0.8 W cm^{-2} (irradiation area = 0.385 cm^2), A is the absorbance of RD SnS NCs aqueous suspension at 785 nm (A = 2.1). where h is the heat transfer coefficient, S is the surface area of the sample vial. hS was calculated to be 3.1 mW/°C by using Eq. 3:

$$hS = \frac{m_D C_D}{\tau_S} \qquad (3)$$

where τ_S is the time constant for heat transfer from the system, m_D is the mass of water (0.1 g) and C_D is heat capacity of water (4.2 J/g·°C). Finally, the heat conversion efficiency (η) of RD SnS NCs can be calculated to be 39.4% according to Eq. 2.

References

1. L. Yuwen, J. Zhou, Y. Zhang, Q. Zhang, J. Shan, Z. Luo, L. Weng, Z. Teng and L. Wang, *Nanoscale*, 2016, **8**, 2720-2726.

2. D. K. Roper, W. Ahn and M. Hoepfner, *J. Phys. Chem. C*, 2007, **111**, 3636-3641.

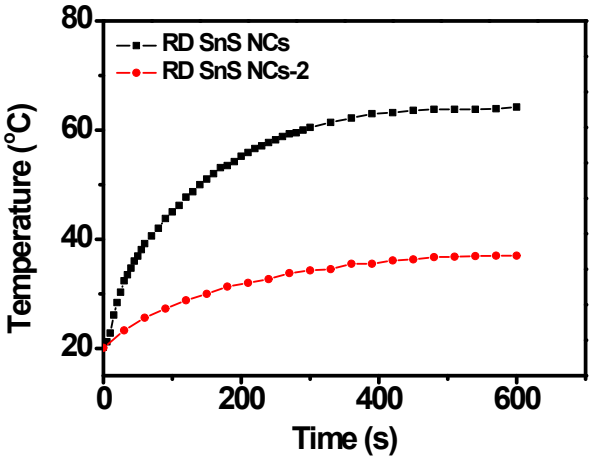

Figure S12. The photothermal heating curves of RD SnS NCs (245±43 nm) and RD SnS NCs-2 (497±34 nm).

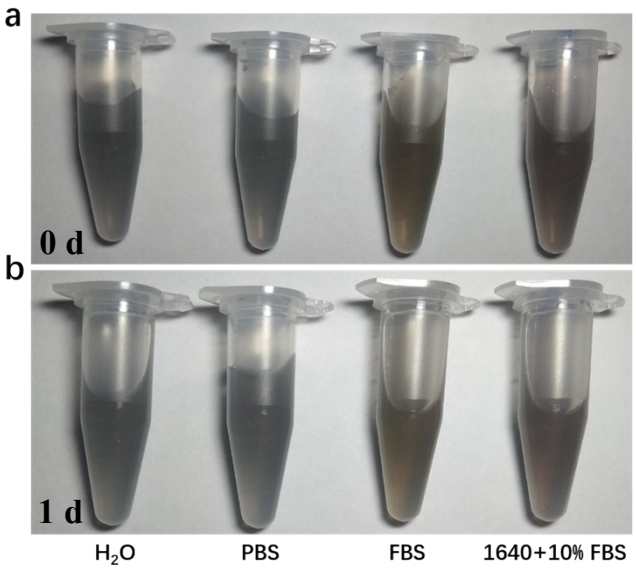

Figure S13. Stability of RD SnS NCs in different mediums. (a) Photographs of RD SnS NC suspension in water, PBS (pH = 7.4, 10 mM), FBS and 1640+10% FBS. (b) Photographs of RD SnS NC suspensions in water, PBS (pH = 7.4, 10 mM), FBS and 1640+10% FBS after they are placed for 1 d. The concentration of RD SnS NCs is 166 μg mL^{-1}.

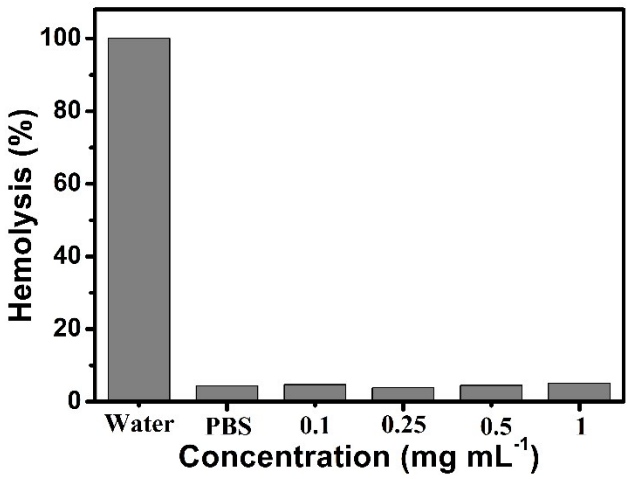

Figure S14. Hemolysis of RD SnS NCs aqueous suspension with different concentration (0.1, 0.25, 0.5 and 1 mg mL^{-1}) in comparison with PBS (pH = 7.4, 10 mM) and water.

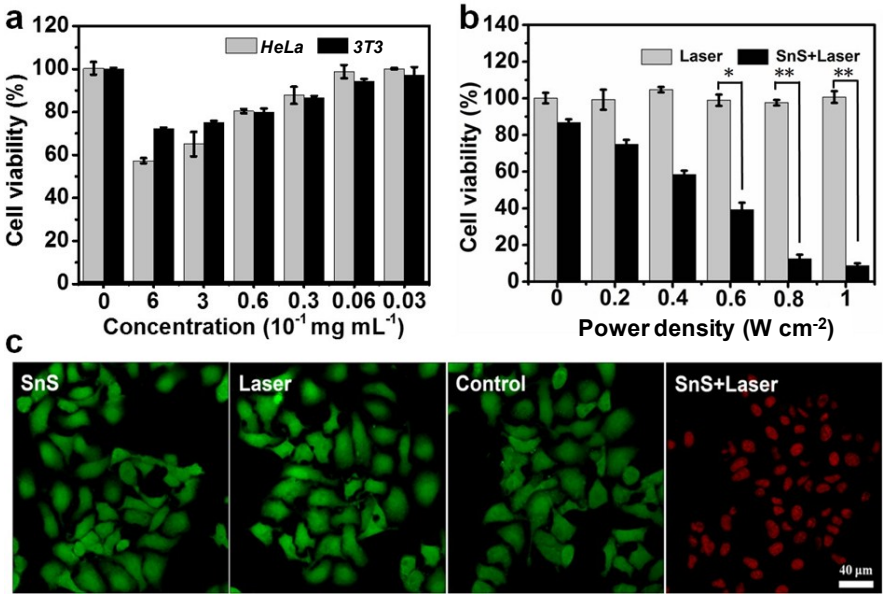

Figure S15. (a) Cytotoxicity of RD SnS NCs against *HeLa* and *3T3* cells without the irradiation of 785 nm laser. (b) Cell viability of *HeLa* cells incubated without or with RD SnS NCs (0.3 mg mL^{-1}) under 785 nm laser irradiation with different power densities for 10 min. $P < 0.05$ is considered statistically significant. *P and **P are less than 0.05 and 0.01 for student's t-test in biological experiments, respectively. (c) Confocal celling imaging using Calcein AM/PI costained to confirm the photothermal effect of RD SnS NCs (0.3 mg mL^{-1}). Calcein AM staining emits green fluorescence, indicating the cell alive, while PI staining emits red fluorescence, indicating the cell dead. The power density of 785 nm laser is 0.8 W cm^{-2}.

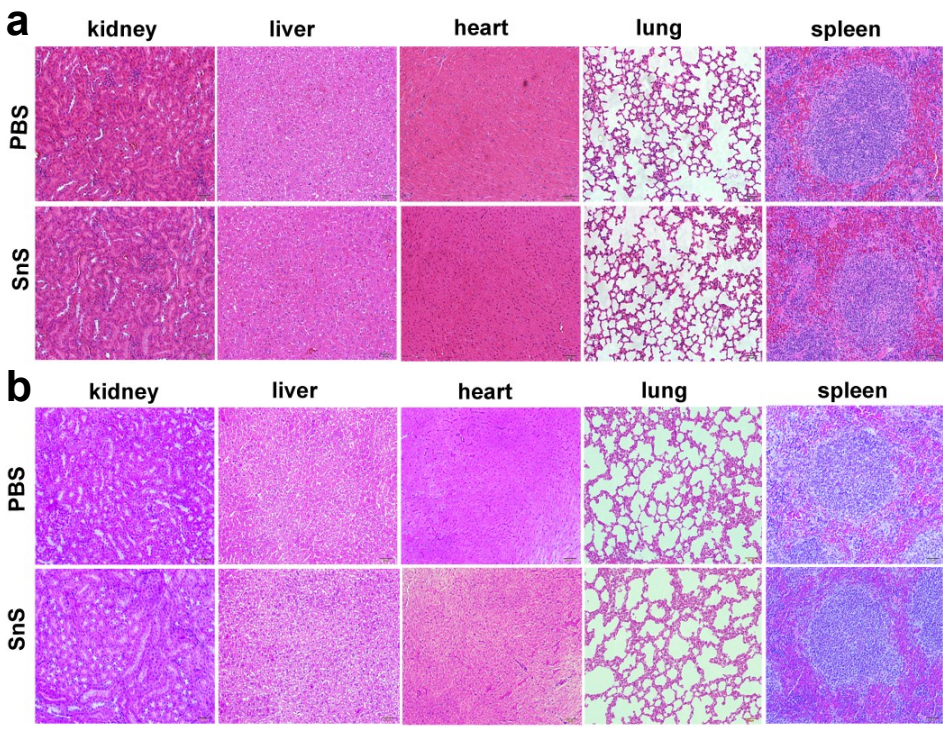

Figure S16. Hematoxylin and eosin stained tissue sections from mice injected with 25 μL of PBS (pH = 7.4, 10 mM) or RD SnS NCs aqueous suspension (2 mg mL^{-1}) for (a) 1 d and (b) 7 d without the irradiation of 785 nm laser. All images are 200 times magnification.

Table S1. Complete blood counts of mice after intravenous injection of 25 μL of RD SnS NCs aqueous suspension (2 mg mL^{-1}) for 1 d.

Item	Control	SnS	Reference range (mean)	Unit
White blood cells	10.2±0.4	9.6±1.0	5.69~14.84 (9.87)	10^9/L
Lymphocyte	7.2±0.6	6.9±0.8	3.6~11.56 (7.29)	10^9/L
Granulocyte	2.7±0.2	2.4±0.3	0.74~3.01 (1.74)	10^9/L
Red blood cells	7.2±0.5	9.4±0.6	8.16~11.69 (9.98)	10^{12}/L
Hemoglobin	125.0±8.5	145.0±7.1	124~189 (154)	g/L
Hematocrit	44.0±2.6	43.9±2.0	43.5~67 (55.4)	%
Blood platelet	737±173	1065±333	476~1644 (963)	10^9/L
Mean corpuscular volume	48.9±0.1	47.0±0.9	50.8~64.1 (55.6)	fL
Mean corpuscular hemoglobin	16.0±0.4	15.5±0.2	13~17.6 (15.5)	pg
Mean corpuscular hemoglobin concentration	328±0.7	329.5±0.7	239~331 (280)	g/L

Healthy Balb/c female mice were sacrificed for blood collection after intravenous injection of RD SnS NCs (dose = 25 mg kg^{-1}) for 1 d. Untreated healthy mice were used as control.